Glass Transition Temperature as a Function of Conversion in Thermosetting Polymers

Arturo Hale*,† **and Christopher W. Macosko**

Department of Chemical Engineering and Materials Science, University of Minnesota, Minneapolis, Minnesota 55455

Harvey E. Bair

AT&T Bell Laboratories, Murray Hill, New Jersey 07974

Received February 21, 1990; Revised Manuscript Received October 3, 1990

ABSTRACT: A simple equation to model the dependence of the glass transition temperature (T_g) on the extent of reaction in highly cross-linked thermosetting polymers has been derived. The model assumes that the increase in T_g is caused by (a) decrease in chain-end concentration, (b) formation of effective cross-links, and (c) further decrease in the configurational entropy due to departure from Gaussian behavior at high cross-link densities. Data of T_g as a function of conversion have been obtained for a multifunctional epoxy–novolac system. This system undergoes a very sharp increase in T_g at high conversions, which can be adequately fit by the model developed here. It has also been found that the change in T_g at low conversions in the multifunctional system can be predicted from data obtained with a model monofunctional system. The equation derived here is compared to several equations published in the literature.

Introduction

Understanding the glass transition temperature (T_g) of thermosetting polymers is very important for various reasons. First and most obvious is that T_g determines an upper bound for the use temperature of the polymer; other reasons include the intimate relationship between the onset of the so-called diffusion control regime during the isothermal cure of a thermoset and its glass transition,[1-7] the influence of T_g on the chemorheology of a thermoset,[8,9] and the correlation between internal stresses and T_g.[10]

Several attempts to correlate the glass transition temperature of cross-linked polymers to their molecular structure have been published.[11-24] The effect of cross-linking on T_g has been studied by using several experimental approaches, including modifying the amount of cross-linker, changing the molecular weight of the prepolymer, altering the stoichiometry, and stopping the reaction at different degrees of conversion. This last case is of great practical importance because it follows the actual curing process; however, this is probably the most difficult case to study because there are many changes taking place simultaneously.

Several authors have reported T_g data as a function of conversion;[2,24-32] most of these data are for epoxy systems. The experimental technique used to obtain the glass transition temperature at different degrees of conversion often consists of interrupting the reaction at different times, usually by quenching, and then scanning the sample to obtain the T_g. The extent of reaction is commonly determined by measuring the residual heat of reaction through differential scanning calorimetry (DSC)[24-27,30] or by spectroscopic analysis, typically infrared spectroscopy;[28,29,32] titration has been used in some cases for ungelled samples.[2,24]

Though several equations to describe the T_g versus conversion data have been utilized in the literature, this can still be considered an unresolved problem, particularly for systems with high cross-link density. Riccardi and co-workers,[27] for example, have limited themselves to fit empirically a polynomial to their data. Other authors[26,28,29] have tried to fit empirically DiBenedetto's equation[13] (eq 1) to the experimental results, with a moderate degree of success:

$$\frac{T_g - T_{g_u}}{T_{g_u}} = \frac{(\epsilon_\infty/\epsilon_0 - c_\infty/c_0)x}{1 - (1 - c_\infty/c_0)x} \tag{1}$$

where x is the cross-link density defined as "the fraction of all segments that are cross-linked",[13] T_{g_u} is the glass transition of the un-cross-linked polymer, ϵ is the lattice energy, c is the segmental mobility, and the subindexes 0 and ∞ refer to the un-cross-linked and the fully cross-linked polymers, respectively. In ref 23, 26, 28, and 29, x has been regarded as the conversion and T_{g_u} as the glass transition of the unreacted system.

A new approach published more recently by DiBenedetto[22] also requires empirical fitting of adjustable parameters. In any case, DiBenedetto has pointed out that the applicability of the principle of corresponding states he used to derive his equation is open to serious question when applied to highly cross-linked systems, because of the great change in configurational entropy introduced by cross-linking.[22]

On the basis of Couchman's approach to model T_g of compatible blends,[33] and the assumption that a cross-linked polymer can be treated as a blend of monomer and completely cross-linked polymer, Pascault and Williams[23] have derived an equation that is mathematically equivalent to eq 1.

A different treatment to describe the variation of T_g during curing has been proposed by Aronhime and Gillham.[34] They assumed that in the pregel region the glass transition is a function of molecular weight only. In the postgel region, they regarded their system as a miscible binary mixture of sol and gel fractions. The T_g of the sol fraction was modeled in a way similar to the T_g of the pregel region, while the T_g of the gel fraction was assumed to increase linearly with cross-link density.

The authors did not compare their relations directly with experimental T_g versus conversion data. They assumed several cases of nth-order kinetics and plotted the theoretical results on a temperature versus (log time

---

† Permanent address: AT&T Bell Laboratories, Murray Hill, NJ 07974.

0024-9297/91/2224-2610$02.50/0

to vitrify) diagram, where they also showed the experimental curve. The qualitative shape of the curve is appropriate, but the fit is rather poor. They argued that the lack of an accurate kinetic model mitigates against a truly good fit between the model and experimental data.

In this work, we present T_g versus conversion data obtained using a polyfunctional novolac epoxy cross-linked with a novolac resin. Although this is not the best model system to test T_g versus conversion relationships because of the low purity and the polydispersity of the starting materials, it was chosen because of its technological importance in the electronics industry, since this type of system forms the basis of molding compounds used in the encapsulation of integrated circuits. The data we present show a very sharp increase in T_g at high conversions, which cannot be adequately fitted by using DiBenedetto's equation (eq 1) in terms of conversion.

Our modeling approach is conceptually similar to that of Aronhime and Gillham,[34] but with some key differences:

(a) The underlying reason for the increase in T_g in the pregel region is assumed to be the drop in chain-end concentration. Although the number-average molecular weight (M_n) is a function of chain-end concentration, it is not convenient to express T_g in terms of M_n in a system with more than two chemical species, since by doing this one would overlook the different contributions to T_g by chain ends with different chemical structures. Therefore, we express T_g in the pregel region as a function of conversion or of chain-end concentration rather than molecular weight.

(b) When considering the postgel region, we do not think it is necessary to break down T_g into a gel contribution and a sol contribution. This would introduce an extra adjustable parameter (the "interaction parameter" Ω in Aronhime and Gillham's paper). We regard T_g as an overall property that is determined by chain-end concentration and cross-link density.

(c) The influence of cross-link density on T_g is assumed to follow DiMarzio's equation (eq 2; see Theoretical Section), rather than a linear function.

(d) The departure from Gaussian behavior at high cross-link densities is taken into account.

By use of the above considerations, a simplified model to describe the variation of T_g with conversion is developed in the Theoretical Section. This model is then applied to describe the experimental results obtained from a novolac-cured epoxy system whose chemistry is well-known.

In order to separate the chain-end effect from the cross-linking effect, a model system consisting of the monofunctional counterparts of the epoxy–novolac resins was studied. The chemical reaction in this model system is exactly the same as that which occurs in the polyfunctional epoxy–novolac system. In the model compound case, however, there is no network formation, and therefore it is not necessary to consider cross-linking effects.

The results from this model compound study are then incorporated into the polyfunctional system, where the effects of cross-linking and non-Gaussian behavior are now taken into account to obtain a relation that describes T_g throughout the whole conversion range.

As this article was being revised, we became aware of the interesting work of Stutz and co-workers in this area.[24] They have successfully modeled the glass transition of cross-linked and un-cross-linked polymers by accounting for the disappearance of chain ends via the Fox–Flory equation (see eq 6) and by using the DiBenedetto equation (eq 1) to describe the effect of cross-link junctions.

Theoretical Section

A rigorous treatment of the glass transition in highly cross-linked systems is a formidable task. If we wish to adopt Gibbs and DiMarzio's configurational entropy approach to define the glass transition[35] (which we consider the most appealing theory from a fundamental standpoint), we encounter the problem of evaluating the partition function of a highly cross-linked system to calculate its configurational entropy. The traditional Flory–Huggins method of counting the number of configurations on a lattice becomes a poor approximation if applied to a highly cross-linked network, because the approximation inherent in the random counting procedure to evaluate the probability of a local cell being empty is not appropriate for highly cross-linked networks.[36]

If we are forced to make simplifying assumptions and introduce empirical parameters to obtain a tractable equation, we could as well aim for a simple-to-use equation and try to minimize the number of empirical parameters.

Using a lattice model and assuming a Gaussian behavior of the chains between cross-links, DiMarzio[12] derived an equation to describe the change in T_g caused by the formation of cross-links. This equation can be expressed as

$$T_g = T_{g_u}/(1 - K_2X) \tag{2}$$

where T_g is the glass transition of the cross-linked polymer, T_{g_u} is the glass transition of an un-cross-linked polymer, which is identical with the cross-linked polymer in every respect except that the cross-links themselves are missing, K_2 is a "universal" constant, and X is a measure of the cross-link density, defined as the moles of chains between cross-links divided by the total number of moles of segments. X can be regarded as the inverse of the number of rotatable bonds per elastic chain.

It should be pointed out that eq 2 was derived for the thermodynamic glass transition (the temperature at which the configurational entropy is zero[12,35]), commonly represented as T_2. In the rest of this work it will be assumed that the behavior of the experimentally measured glass transition T_g parallels that of the thermodynamic T_2,[12] that is, that both quantities follow the same functionality with respect to conversion. The validity of this assumption will be the subject of another work. Equation 2 is strictly valid only for low cross-link densities, since its derivation assumes that the chains between cross-links are long enough to obey a Gaussian behavior. In our case, the distance between cross-links at high conversions is that of only a few bonds, so the chains are not expected to be Gaussian.

For networks of such short chains, therefore, a non-Gaussian treatment is necessary for a rigorous representation of their statistical mechanical behavior. Charlesworth[21] was probably the first researcher to attempt this treatment in order to describe the glass transition temperature in highly cross-linked systems. In a study of amine-cured epoxies, he accounted for the non-Gaussian behavior by utilizing an inverse Langevin distribution. He actually used what is now known as the "incorrect Langevin distribution",[37] claiming that it provides a more accurate representation of the behavior of short chains than the correct inverse Langevin distribution. It is questionable, however, that this treatment is really an improvement over the Gaussian treatment. The inverse Langevin distribution was originally derived as a result of the failure of the Gaussian model to take into account the finite extensibility of the polymer chains;[38] hence the inverse Langevin distribution does a better job than the

Gaussian model in describing the behavior of chains at high extension ratios.[37,39] At low extension ratios, however, the Gaussian approximation is better than the inverse Langevin function, even for chains as short as four bonds![37] The inadequacy of the inverse Langevin distribution is caused by the grave approximations incurred in its derivation.[37] In fact, Flory suggested that, in view of the forfeiture of rigor through these approximations, the inverse Langevin distribution function should perhaps be relegated to the status of an empirical representation of the distribution.[37] In the end, Charlesworth[21] had to resort to the use of two adjustable parameters.

Unfortunately, the attempt to replace the Gaussian statistical theory by a more exact treatment involves a considerable sacrifice of both simplicity and generality.[39] If one wants to improve over the inverse Langevin function to describe the configurational statistics of short chains, a great more deal of complexity in the model is necessary. Hill and Stepto[40] and Mark and Curro[41] have applied the rotational isomeric state model to describe the non-Gaussian behavior of short chains. This approach requires the use of computational methods for evaluating the moments of the distribution,[40] or Monte Carlo calculations to simulate spatial configurations of the chains.[41] In addition, the results obtained are unique to the particular polymer under study. This technique is not easily applicable to polymers with complex chemical structures, such as epoxy resins.[42]

A further cause of departure from ideality, besides non-Gaussian behavior, has been suggested to arise from steric restrictions on the freedom of chain segments in the proximity of junctions.[21,42] The net effect of both the non-Gaussian behavior of the short chains and the steric interactions is a decrease in the configurational entropy over the value that would be expected from the Gaussian case. Our aim is to account in a simple way for this decrease in the configurational entropy in the development of a T_g equation that includes the effect of these nonidealities. This will be done by using an empirical function to describe the influence of the nonidealities on the configurational entropy. Although we are not aware of any experimental data describing the change in the configurational entropy as one departs from Gaussian behavior, a phenomenological functional form can be obtained from rubber elasticity data. Charlesworth[42] has used eq 3 successfully

$$G = \phi\nu\rho RT/(1 - \psi\nu^2) \tag{3}$$

to describe the dependence of shear modulus on cross-link density for highly cross-linked epoxies, where G is the shear modulus, ν is the moles of elastically active network strands per unit volume, ϕ is the front factor, ρ is the polymer density, R is the gas constant, T is the absolute temperature, and ψ is an empirical constant that lumps together the effect of the nonidealities. We have left out of the above equation the contribution of trapped entanglements for simplicity, because it is not relevant to our discussion.

Equation 3 differs from the equation of ideal rubber elasticity by the factor $1/(1 - \psi\nu^2)$. If we carry this factor backwards through the derivation of the ideal rubber elasticity equation to obtain an expression for the configurational entropy, we obtain

$$\Omega(\text{non-Gaussian}) = \Omega(\text{Gaussian})^{1/(1-\psi\nu^2)} \tag{4}$$

where Ω is the probability distribution function describing the number of ways to arrange a chain whose ends are tied down to given cells in the lattice. The effect of the exponent $1/(1 - \psi\nu^2)$ is to decrease the number of configurations, therefore lowering the configurational entropy. An additional effect of using this functional form is the narrowing of the distribution of end-to-end distances. Both of these effects are qualitatively correct, since with stiffer chains one would expect both a lower number of configurations and a lower probability of large fluctuations away from the favored configurations. By use of eq 4 in DiMarzio's derivation[12] of eq 2, the latter becomes

$$T_g = \frac{T_{g_u}}{1 - \dfrac{K_2X}{1 - \Psi X^2}} \tag{5}$$

where Ψ is an empirical constant that lumps together the effects of nonidealities such as non-Gaussian behavior and steric effects on the chain configurations of highly cross-linked systems. There is not enough information available to determine whether all the simplifying assumptions DiMarzio used in his derivation are valid here; however, failure to use these assumptions would only introduce more unknown parameters.

The definition of cross-link density is not a trivial matter in relation to T_g theories. Should one use branch points, or elastically effective cross-links? This question is irrelevant in the case of fully reacted stoichiometric mixtures, because every branch point is an elastically effective cross-link. The same is true for long linear chains to which a cross-linker is added (such as vulcanization of rubber), since these systems gel with very small amounts of cross-linker.[43] Nevertheless, the answer is not obvious in the case of a polymerizing network, which forms many branch points from the very beginning of the reaction, but which does not generate elastically effective cross-links until after the gel point. As Stutz and co-workers correctly point out,[24] T_g has been experimentally shown to be a short-range phenomenon, so it should not matter whether a cross-link is elastically effective or not, since this definition of a cross-link would involve a long-range effect. For instance, Boyer[44] has suggested that the glass transition is associated with a coordinated segmental motion of 10–20 of the chain backbone atoms, a rather local phenomenon. On the other hand, if we adopt the configurational entropy approach, the formation of an elastically effective cross-link should decrease the configurational entropy (and therefore increase the glass transition), because the fact that the elastically effective cross-link is attached to the network implies that it can be placed in a lattice in many fewer ways than an ineffective branch point. Experimental data can be invoked to justify each point of view. Stutz and colleagues claimed that the fact that the T_g versus conversion curve departs from linearity before the gel point in their epoxy–amine system proves that branch points rather than effective cross-links affect T_g.[24] There are, however, other ways to explain this curvature (see derivation of eq 10 and eq 15). On the other hand, there are data that show a more accelerated increase in T_g after the gel point,[29,31,32] suggesting that the elastically effective cross-links have an influence on the glass transition. The two views can probably be reconciled by resorting to the Adam–Gibbs theory.[45] According to this theory, the actual size of the cooperative region involved in the glass transition is dependent on the time scale of the experiment: the longer the time scale, the larger the number of segments involved in the cooperative transition, until ultimately at infinite time the cooperative region will comprise the whole sample. Hence the true glass transition viewed as a thermodynamic transition[35] is a long-range phenomenon comprising the whole sample, and therefore it *does* matter whether a cross-link is elastically effective. The short-range nature of T_g observed experimentally is due to the finite time scale of the experiments. In this work we shall use elastically effective cross-links in the determination of cross-link density X, in order to be consistent with the lattice model adopted. However, this choice is not critical in terms of obtaining a good fit.

It is now necessary to find an expression for T_{g_u} as a function of extent of reaction. T_{g_u} has been defined as the glass transition of an un-cross-linked polymer that is identical with the cross-linked polymer in every respect except that the cross-links themselves are missing. Therefore the change in T_g as the system reacts and the chains grow should be included in T_{g_u}. The only effect that is not included in T_{g_u} is the decrease in configurational entropy that arises from the formation of effective cross-links. Although it is possible to derive an equation for T_{g_u} based on the Gibbs–DiMarzio configurational entropy theory,[35] such an approach would yield a nonexplicit equation requiring two unknown parameters: a hole energy parameter and a flex energy parameter. We consider that such approach is not really necessary in this work, in particular since there are very simple equations that have been used successfully in the literature to describe the glass transition temperature in non-cross-linked systems, such as[46]

$$T_g = T_{g_\infty} - K/M \tag{6}$$

or[47]

$$1/T_g = 1/T_{g_\infty} + K'[1/M] \tag{7}$$

where T_g is the glass transition temperature of a linear polymer of molecular weight M, T_{g_∞} is the hypothetical glass transition of an infinitely long linear polymer, and K and K' are constants. It is well-known that eq 6 is limited to high molecular weight polymers for which the weight fraction of the end groups is small,[46,48] while eq 7 is much more appropriate for describing T_g down to low molecular weights.[47] For this reason the latter will be used in this work.

Since the thermosetting systems under consideration start branching from the beginning of the reaction, one should also worry about the effect of the branch points (junctions) on the glass transition. When a branched molecule is compared with a linear molecule of the same molecular weight, two opposing effects can be identified: the additional number of chain ends in the branched molecule would cause its T_g to decrease, while the restriction in mobility caused by the junction point would increase T_g. There is no doubt that as a three-way junction is formed the glass transition increases. The question is whether this increase is caused only by the loss in mobility that accompanies the formation of a covalent bond (and therefore is indistinguishable from the increase in T_g brought about by chain extension as two chain ends react), or whether there is an additional increase due to the mere fact that the new covalent bond formed is now part of a three-way junction. It is not clear which of these instances is correct, since the data available in the literature are contradictory. On the one hand, it has been shown that glass transition temperatures of star polystyrenes follow quantitatively the end-group concentration dependence established for linear polymers without taking into account the effect of the central branch point.[48] Meares has observed the same behavior on branched polyvinyl acetates.[49] On the other hand, Rietsch and co-workers have published data from polystyrene stars showing a higher T_g for the branched samples,[16] indicating that the effect of the junction is more important than the effect of the chain ends. The key difference between the data of Roovers and Toporowski[48] and that of Rietsch and collaborators[16] is the chemical structure of the junctions. The former obtained well-defined junctions by direct coupling of a tetrafunctional agent (1,2-bis(methyldichlorosilyl)ethane) with four living polystyrene chains;[50] on the other hand, Rietsch and co-workers used a system where the junctions consist of poly(divinylbenzene) nodules. The number of branches in this system is harder to control, since it depends on several factors: the ratio of divinylbenzene to polystyrene, the molecular weight of the linear precursors, and the global concentration.[51,52] The higher T_g values observed with this system may be caused by the fact that this is actually a polystyrene–poly(divinylbenzene) copolymer.

As suggested by Meares[49] and Roovers and Toporowski,[48] we shall assume that the glass transition temperature in a branching un-cross-linked polymerizing system is determined by the concentration of end groups. The validity of this assumption will be corroborated in the Experimental Section. Equation 7 can then be expressed as

$$\frac{1}{T_{g_u}} = \frac{1}{T_{g_\infty}} + K''[\text{C.E.}] \tag{8}$$

where [C.E] is the concentration of chain ends, and T_{g_u} is the glass transition of the un-cross-linked branched system.

In this work we consider any site that has the potential to form a new covalent bond to be a "chain end". Therefore, strictly speaking, if there are chain ends of different chemical structures, eq 8 should more properly be stated as

$$\frac{1}{T_{g_u}} = \frac{1}{T_{g_\infty}} + K_1''[\text{C.E.}_1] + K_2''[\text{C.E.}_2] + \ldots \tag{9}$$

where the subindexes 1 and 2 refer to the different structures of the chain ends, and ∞ refers to an infinitely long polymer with no chain ends. In the case of an epoxy–amine reaction, there would be three different types of "chain ends": epoxides, primary amines, and secondary amines. A reaction between an epoxide and a primary amine would extend the linear chain, while the reaction of a secondary amine would form a branch point. With this approach it is not necessary to include the possible effect of branching as a separate term, since it is accounted for by regarding secondary amines as one more kind of chain end with its own contribution to T_g independent from epoxides and primary amines. For a stoichiometric mixture of chain ends of type 1 reacting with chains ends of type 2 (and no other reactions), $[\text{C.E.}_1] = [\text{C.E.}_2]$ at all times, and eq 9 reduces to eq 8. This condition will be assumed for the rest of this work.

In terms of extent of reaction, eq 8 can be expressed as

$$\frac{1}{T_{g_u}} = \frac{1}{T_{g_0}} - k\xi \tag{10}$$

where T_{g_0} is the glass transition of the unreacted monomeric mixture, and ξ is the conversion or extent of reaction. If the stoichiometry is not balanced, ξ represents the conversion of the limiting reagent, and T_{g_0} will depend on the stoichiometry. Equation 10 is more convenient to use than eq 8, since T_{g_0} is a readily measurable quantity, as opposed to the hypothetical nature of T_{g_∞}.

Equation 10 represents the increase in T_g due only to the decrease in chain-end concentration. Inserting this equation into eq 5, we obtain an expression that accounts

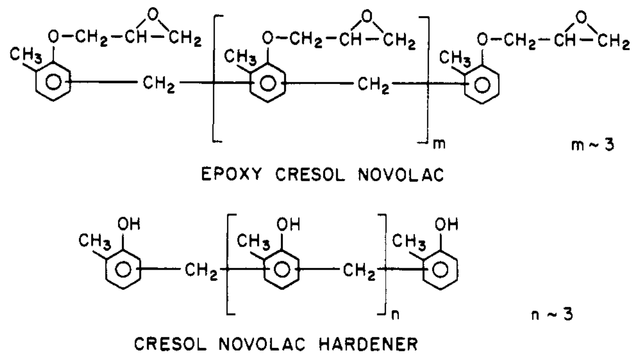

Figure 1. Molecular structure of epoxy cresol novolac and of cresol novolac hardener.

for the change in T_g due to the combined effects of decreasing chain-end concentration, formation of cross-links and departure from Gaussian behavior at high cross-link densities:

$$T_g = \frac{\left(\dfrac{1}{\dfrac{1}{T_{g_0}} - k\xi}\right)}{1 - \dfrac{K_2X}{1 - \Psi X^2}} \qquad (11)$$

where T_g is the glass transition of the thermosetting polymer, T_{g_0} is the glass transition of the unreacted mixture, ξ is the extent of reaction, k incorporates the effect of chain ends, K_2 is DiMarzio's constant originally thought to be "universal"[12] (this constant has been shown to vary for different chemical systems[53,54]), X is a measure of the cross-link density defined as the moles of chains per mole of segments, and Ψ is an empirical constant that lumps together the effects of nonidealities such as non-Gaussian behavior and steric effects on the chain configurations of highly cross-linked systems. The influence of the functionality of a cross-link on the mobility of a chain is accounted for implicitly in the calculation of X by weighting differently the cross-links of different functionalities as explained elsewhere.[55,56]

Experimental Section

Materials. The model compounds employed were phenyl glycidyl ether (Aldrich, 99%; epoxy equivalent 150 g/equiv), and *o*-cresol (Aldrich, 99+%). The accelerator was 2-ethyl-4-methylimidazole (Aldrich, 99%). The polyfunctional epoxy resin used was an epoxy cresol novolac supplied by Ciba-Geigy (Araldite ECN-1273; epoxy equivalent 215 g/equiv, number-average functionality 4.8); the cresol novolac hardener was Ciba-Geigy Araldite HT-9490; number-average functionality 5.1, hydroxyl equivalent 126 g/equiv. All the epoxy equivalents were determined by titration (ASTM-D1652). The rest of the information was provided by the suppliers. The chemicals were used as received. Figure 1 shows the idealized structures of the resin and the hardener.

The equivalent weights obtained experimentally are somewhat higher than the values expected from the structural formulas depicted in Figure 1 because of the presence of other species generated during the synthesis of these resins. In the case of epoxies, these species consist of chlorohydrins (produced by incomplete dehydrohalogenation), oligomers (formed by the reaction of an unreacted phenolic hydroxyl with an epoxy group), and homopolymers (formed when two epoxy groups react with each other).[57] All these byproducts are considerably less reactive toward epoxides than the phenolic hydroxyls of the curing agent, and therefore, their presence is not expected to affect the network buildup chemistry.

Instrumentation. DSC. The glass transition temperatures of the model compounds were determined by using a Mettler 3000 DSC calibrated with high-purity indium (high temperatures) and high-purity (HPLC grade) *n*-heptane at low temperatures. A Perkin-Elmer DSC-2 connected to a 3600 TADS data station was used to study the variation of the glass transition temperature (T_g) as a function of conversion in the polymeric system. This instrument was calibrated with high-purity indium and zinc.

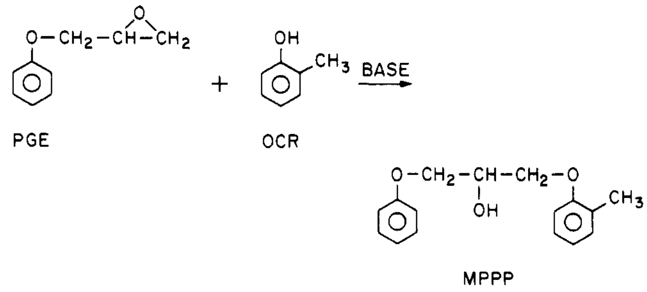

Figure 2. Reaction between phenyl glycidyl ether (PGE) and *o*-cresol (OCR) to form 1-(2-methylphenoxy)-3-phenoxy-2-propanol (MPPP).

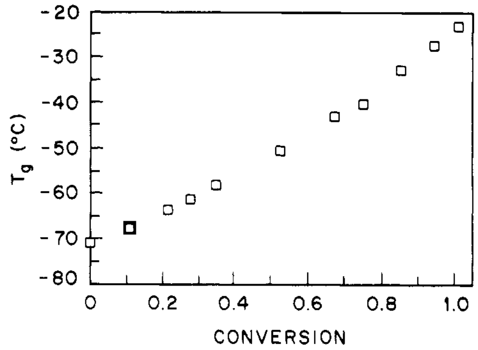

Figure 3. Glass transition as a function of extent of reaction for a phenyl glycidyl ether–*o*-cresol system.

NMR. The solid-state NMR spectra are obtained in a modified Nicolet NT-150WB spectrometer with magic angle spin and cross polarization capabilities, utilizing a contact time of 2 ms and a repetition time of 10 s. The number of scans was 176.

Procedure and Results. (i) Model Compounds. Phenyl glycidyl ether (PGE) and *o*-cresol (OCR) were employed for this study. These compounds are monofunctional counterparts of the epoxy cresol novolac and cresol novolac hardener, respectively. As we have shown,[58] stoichiometric amounts of PGE and OCR in the presence of 2-ethyl-4-methylimidazole will react cleanly to form 1-(2-methylphenoxy)-3-phenoxy-2-propanol (MPPP) (Figure 2). There is no branch formation in this reaction; a "dimer" is formed from two monomers. Thus, MPPP was prepared by reacting a stoichiometric mixture of PGE and OCR. The T_g was studied as a function of conversion in the model system (PGE–OCR). Since there is always some error in the measurement of conversion of chemical groups, an alternate method to prepare the samples was employed to avoid this problem. First we note that a mixture of initially 1 mol of PGE and 1 mol of OCR that have reacted up to an extent of reaction ξ will consist of $1 - \xi$ mol of PGE, $1 - \xi$ mol of OCR, and ξ mol of MPPP. Instead of obtaining such a partially reacted mixture by reacting PGE with OCR, stopping the reaction, and then measuring conversion, the sample was made by mixing PGE with OCR and MPPP in the ratio $(1 - \xi):(1 - \xi):\xi$. MPPP had been synthesized as described above. This procedure provided us with a much more accurate way of controlling the "conversion". The samples thus obtained were scanned in the DSC from −120 to 20 °C to measure the glass transition temperatures.

The variation of T_g as a function of conversion for the model compounds is shown in Figure 3.

(ii) Polyfunctional System. Stoichiometric amounts of resin and hardener were dissolved in methylene chloride together with 0.74 wt % of imidazole accelerator, and then vacuum was applied in order to remove the methylene chloride, until constant weight was achieved. This procedure for mixing the reactants was chosen

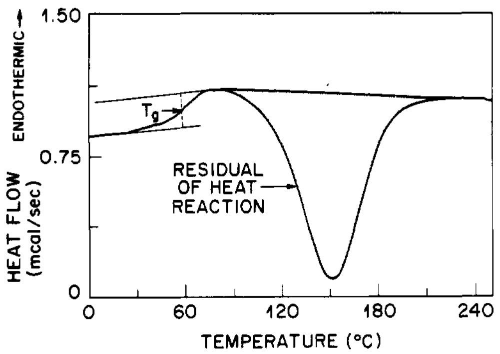

Figure 4. Typical DSC scan showing the glass transition temperature and the residual heat of reaction. This particular run corresponds to an epoxy-novolac that had previously reacted for 10 min at 100 °C.

rather than melting them in order to avoid chemical reaction during mixing. The mixture was then cured in a Perkin-Elmer DSC-2 differential scanning calorimeter connected to a TADS-3600 data station. Each sample was cured isothermally for a certain amount of time, quenched, and rescanned from room temperature to 280 °C at 20 °C/min to obtain the glass transition temperature and the residual heat of reaction. The glass transition values reported here are the "midpoint" T_g's, i.e., the temperature at which the step increment in C_p reaches half of the total ΔC_p value (ΔC_p is the difference in specific heat between the glassy and the rubbery states). The reproducibility of the T_g measurements is ±1.5 °C. The extent of reaction was calculated from the residual heat of reaction, as we shall describe later. Curing temperatures between 100 and 160 °C were utilized. Since the reaction is thermally activated, cooling the sample to room temperature or below is an effective way of stopping the reaction. Figure 4 shows a DSC trace of a dynamic run scanning a sample that had been partially reacted previously. The glass transition temperature and the exotherm following it can be observed; the base line was determined by drawing a straight line between the onset and the end of the exotherm in such a way that the baseline is tangent to the DSC curve at those two points. The whole procedure was repeated for several samples using different temperatures and cure times.

Samples that were cured for long times at a given temperature showed signs of physical aging. Physical aging consists of a densification process, which is inherent in the nonequilibrium character of the glassy state.[59] Any glass will spontaneously densify as it tries to approach equilibrium. The rate of densification increases as T_g is approached from below. In the samples we cured for long times, T_g increased with extent of reaction until it became higher than the reaction temperature. At this point the sample became glassy, but its temperature was still close enough to T_g to permit rapid aging. When the sample is scanned in the DSC, the effect of aging can be seen as an endothermic peak caused by enthalpic relaxation. Once an aged sample is heated above T_g, the high mobility "erases" the memory. If this sample is then quenched from above T_g to a low temperature, and a rapid heating scan is performed in the DSC, the enthalpic relaxation peak will no longer appear.[60] Figure 5 shows a first scan of an aged sample, together with a second scan of the same sample. The enthalpic relaxation peak has been erased. It is obvious from Figure 5 that significant error could be incurred by trying to obtain the residual heat of reaction from an aged sample. To avoid this difficulty, the DSC scan of every aged sample was stopped immediately at the end of the relaxation peak to "erase" this aging effect, the sample was quenched, and a second scan was performed. Even if some reaction takes place during this procedure, it is not relevant, since it is accounted for in the way we calculate conversion (see below). An alternate procedure to measure the residual heat of reaction of aged samples has been reported;[30] this method needs only one DSC scan per measurement, but it requires knowledge of the ΔC_p value as a function of conversion.

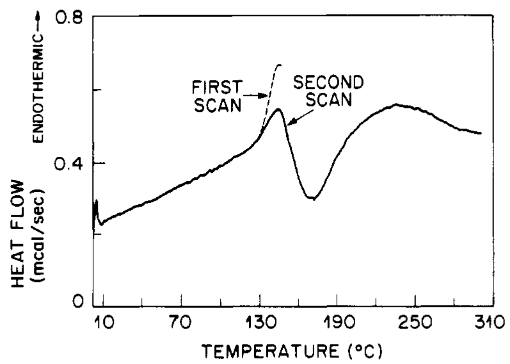

Figure 5. DSC scan of an epoxy-novolac that had previously reacted for 60 min at 120 °C. The first scan shows an enthalpic relaxation peak due to aging. The run was stopped immediately after the maximum of the peak was reached, and the sample was quenched and rescanned. The second scan shows that the aging effect has been erased.

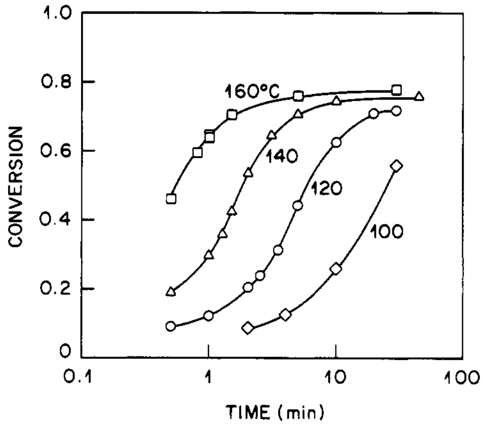

Figure 6. Extent of reaction as a function of curing time for our epoxy-novolac system. The cure temperature is shown on each curve.

Another sample was cured dynamically from room temperature to 280 °C with a heating rate of 20 °C/min. The integration of this exotherm supplied the maximum heat that can be detected from reacting our samples in the DSC at 20 °C/min. This "maximum heat" is not expected to be the total heat of reaction, since the lower mobility as T_g rises prevents the reactive groups from reacting completely within the time frame of the experiment. Taking this into account, the extent of reaction ξ can be calculated from

$$\xi = \frac{\Delta H_U - \Delta H_R}{\Delta H_T} + \xi_0 \qquad (12)$$

where ΔH_R is the residual heat of reaction obtained from rescanning the partially reacted sample, ΔH_U is the heat of reaction evolved by an "unreacted" sample (i.e., the maximum heat that can be detected from reacting our samples in the DSC at 20 °C/min), ΔH_T is the total heat evolved by an epoxide-phenol reaction, determined from model compounds to be -20.7 kcal/equiv mol,[58] and ξ_0 is the initial extent of reaction in the "unreacted" sample, which in this work was found to be 2% by titration with HBr (ASTM D-1652). The fact that the enthalpy of the epoxide-phenol reaction is lower than that of the epoxide-amine reaction (-26.3 kcal/mol)[61] is not surprising. A simple calculation using a group contribution method to estimate heats of formation[62] shows that the transformation of a phenol into an ether is ~4 kcal/mol more endothermic than the change of a primary amine into a secondary amine.

The variation of conversion with time under four isothermal conditions is shown in Figure 6. The error bars for the conversion values are ±0.02. It can be seen that conversion reaches apparent limiting values, and that these limiting values increase with cure temperature. The leveling off of conversion coincides with the region where the glass transition temperature becomes comparable to the reaction temperature. These apparent limiting values of conversion are due to the reaction becoming diffusion controlled

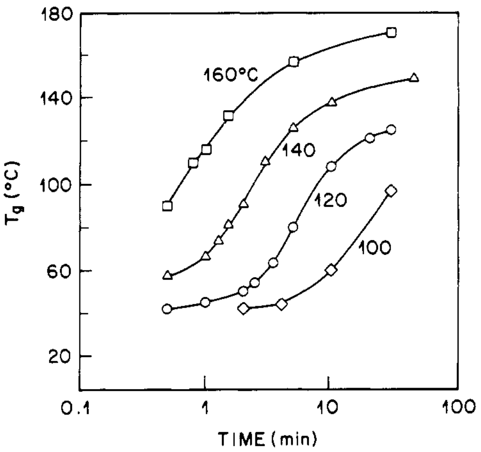

Figure 7. Glass transition as a function of curing time for our epoxy–novolac system. The cure temperature is shown on each curve.

Table I
Glass Transition Temperature as a Function of Conversion for the Epoxy–Novolac System

conversion	T_g, °C	conversion	T_g, °C	conversion	T_g, °C
0.02	37	0.36	74	0.65	110
0.09	42	0.43	81	0.71	131
0.09	42	0.44	79	0.71	120
0.12	45	0.46	90	0.71	126
0.13	45	0.54	91	0.72	124
0.19	57	0.56	97	0.74	124
0.21	50	0.60	109	0.75	138
0.24	54	0.63	108	0.76	148
0.26	60	0.64	112	0.78	169
0.30	67	0.64	115	0.78	173
0.32	63				

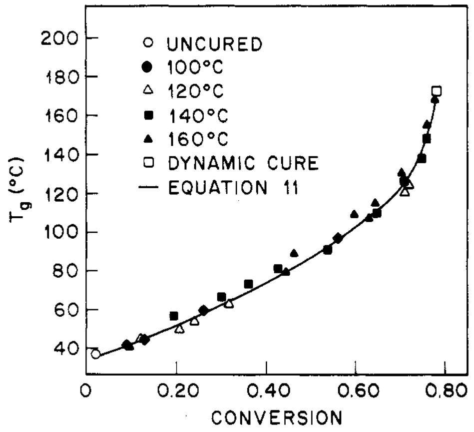

Figure 8. Glass transition as a function of extent of reaction for our epoxy–novolac system. The legend shows the temperatures at which the samples were cured. The "dynamic" cure was performed by heating the sample from room temperature to 280 °C at a controlled rate of 20 °C/min. The continuous line was calculated with eq 11.

as T_g approaches the cure temperature.

Figure 7 displays the change in T_g as a function of cure time. Initially there is a sharp increase in T_g due to the fast reaction kinetics. The rate of increase of T_g with time drops abruptly when T_g is comparable to the reaction temperature. This indicates that when T_g approaches the reaction temperature, the sample vitrifies and the reaction becomes diffusion controlled. It should be stressed that the reaction does not stop; it continues, though at a slower rate. This behavior has been discussed in the literature.[6,7,30]

Table I lists the glass transition temperature values obtained as a function of conversion. Figure 8 displays these values for the different cure temperatures. Within the experimental scatter, all the values collapse to a single curve, which, in agreement with Lunak et al.,[2] means that the glass transition is a function of conversion only, and not of cure temperature. A key feature in this figure is the sharp increase in T_g at high conversions. It should be noted that the highest value of T_g shown in Figure 8 is a reproducible result obtained from several runs. In addition we show the values of ΔC_p in terms of conversion in Figure 9. Although the ΔC_p values are very scattered, it is clear that they are approximately constant at low conversions, showing a steady and significant decrease thereafter.

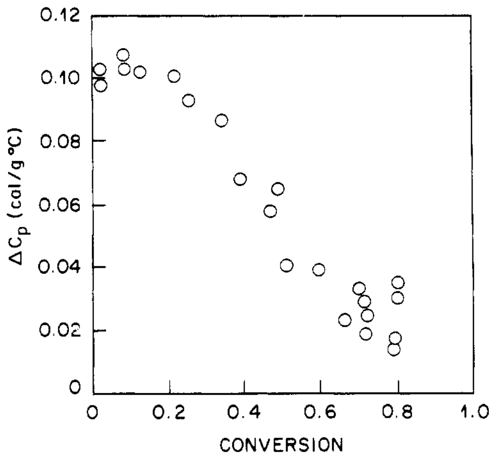

Figure 9. ΔC_p as a function of extent of reaction for our epoxy–novolac system.

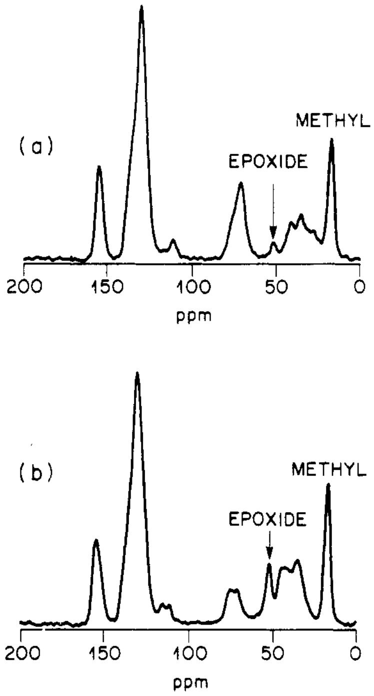

Figure 10. Cross-polarization magic angle spin ^{13}C NMR spectra of a stoichiometric epoxy–novolac mixture. (a) Spectrum of a sample that had been cured for 1 h at 180 °C, and whose glass transition temperature is 183 °C. The peak at 52 ppm shows that a significant amount of unreacted epoxides is still present. (b) Spectrum of an unreacted mixture.

There is one potentially controversial issue that must be addressed. The highest value of conversion we recorded after a dynamic scan in the DSC is nearly 80%. The value of the (midpoint) glass transition at this conversion is 173 °C. It may seem hard to believe that 20% of the original reactive groups have not reacted. It could be argued that the DSC is not sensitive enough to detect the last 20% of reaction, and that in fact the reaction proceeds almost to completion. However, solid-state ^{13}C NMR spectroscopy supports the conclusion that there is a significant amount of unreacted groups. Figure 10a shows a cross-polarization magic angle spin ^{13}C NMR spectrum of a sample

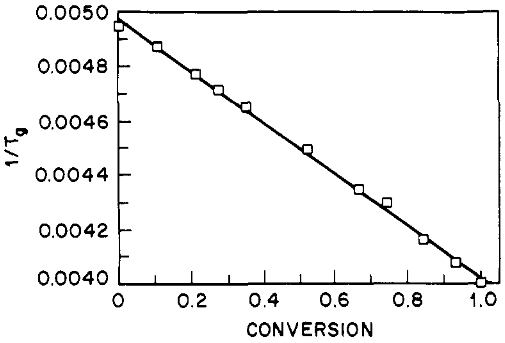

Figure 11. Inverse of the glass transition as a function of extent of reaction for a phenyl glycidyl ether-o-cresol system. Data from Figure 3.

whose T_g was 183 °C. This sample had been cured in an oven for 1 h at 180 °C. Figure 10b shows an equivalent spectrum of an unreacted mixture for comparison. The spectrum of the reacted sample shows a significant amount of unreacted epoxides (52 ppm). Although one cannot expect to obtain accurate quantitative results from a CP-MAS ^{13}C NMR spectrum without carefully controlling the experimental parameters and determining the optimum instrumental settings, we can obtain a very rough estimate of the amount of unreacted epoxies by taking the ratio of the intensity of this peak to the intensity of an invariant peak and then comparing this ratio to that obtained from the unreacted sample. With the methyl peak (17ppm) as an internal standard, this procedure yields a value of ~30% unreacted epoxies. This value should be regarded as a rough approximation. What is clear is that there is a significant amount of epoxides left, which is consistent with the 80% conversion measured with the DSC for a similar sample. This value of 80% conversion should *not* be regarded as an ultimate conversion. It is simply the maximum conversion we can *measure* within the time it takes to heat a sample in the DSC from room temperature to 280 °C. Higher conversions can be achieved, as exemplified by a glass transition temperature of 190 °C obtained after curing for 36 h at 235 °C. Extrapolating from Figure 8, it seems that this T_g would correspond to a conversion lower than 85%. Achieving complete conversion may not even be possible within a reasonable time scale. Even at 235 °C, the curing reaction is very slow in its final stages, due to both the low concentration of remaining reactive groups and the low mobility as the glass transition temperature approaches the curing temperature. Besides, maintaining the sample at these high temperatures for extended periods of time will cause chemical degradation to occur. Aside from time-scale limitations, the concept of an intrinsic ultimate conversion lower than 100% is not unreasonable. It has been suggested that during the latest stages of the reaction in a network polymer the unreacted groups are spatially separated from each other and cannot meet and react due to the high connectivity of the network.[63] Computer modeling predicts a topological limit for the conversion in an epoxy-amine system of $\xi = 0.95-0.96$.[63] Our chemical system has a much higher functionality than amine-cured diepoxies, so it is not surprising to expect lower ultimate conversion values caused by more severe topological limitations.

Discussion

Application to the Epoxy-Novolac System. If it is true that the increase in T_g can be described by the decrease in chain-end concentration as long as no elastically effective cross-links are formed, then the increase in T_g caused by the reaction of two groups in a *branching* molecule before gelation should be the same as the increase in T_g caused by the reaction of the same reactive groups in a *nonbranching* system.

Figure 11 displays a plot of $1/T_g$ in terms of conversion for our model system consisting of monofunctional compounds. The linearity of this graph demonstrates that eq 10 describes our model compounds data adequately. The value of k is 9.513×10^{-4}.

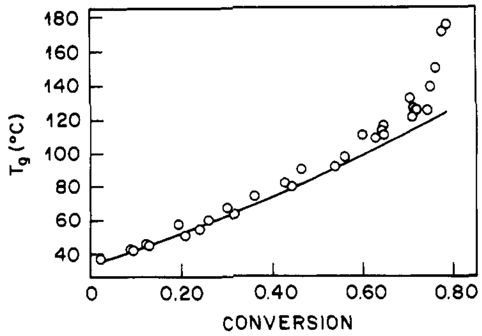

Figure 12. Glass transition as a function of extent of reaction for our epoxy-novolac system. The symbols represent experimental data from Figure 8. The continuous line represents the predicted glass transition temperature in the absence of cross-links from Equation 13.

Now we have to determine whether this value of k can be applied to the data of the *polyfunctional* system. Figure 12 shows again the data of our polyfunctional system from Figure 8. The continuous line is a plot of the equation

$$y = 1/(0.00327 - 9.513 \times 10^{-4}\xi) \tag{13}$$

which can also be expressed as

$$\frac{1}{y} = \frac{1}{T_{g_0}} - 9.513 \times 10^{-4}\xi \tag{14}$$

where T_{g_0} is the glass transition of the unreacted mixture. Thus, eq 10, which was used to model T_g versus conversion of model *monofunctional* compounds, can be applied to describe the T_g change with conversion in our *polyfunctional* resin (except for high conversions) *using the same slope* (-9.513×10^{-4}). This implies that, with the exception of high conversions, the increase in T_g with extent of reaction in the polyfunctional resins is caused by the same mechanism as in the monofunctional compounds, that is, the reduction of the concentration of chain ends.

It should be stressed that this ability to predict T_g as a function of conversion (at low conversions) in the polyfunctional system using a parameter determined *independently* for model monofunctional compounds only works when a reciprocal T_g function is used (eq 10). The same success is not achieved if a linear relation is employed: the slope of the T_g versus ξ curve is *not* the same as in the monofunctional and polyfunctional systems. This is a consequence of the fact that the linear equation (eq 6) is not appropriate for low molecular weights.

We do not really expect that T_g in a highly cross-linked polymer can be explained only in terms of chain ends. The departure of the experimental data from the continuous line in Figure 12 must be due to the reduced configurational entropy caused by the formation of elastically effective cross-links. Before proceeding any further we should point out that the possibility of a second reaction taking place can be ruled out for the particular case of our chemical system at stoichiometric balance, as we have shown in our earlier work.[58]

The cross-link density X was calculated by using a statistical model[56] as described elsewhere.[54] In this calculation the polydisperse epoxy monomer was approximated by a binary mixture of four-functional and five-functional monomers, keeping the same average functionality. Similarly, the novolac hardener was considered as a mixture of five-functional and six-functional monomers. Although the step-growth polymerization involved in the novolac chemistry leads to a broad distribution closer to a most probable rather than to a monodisperse

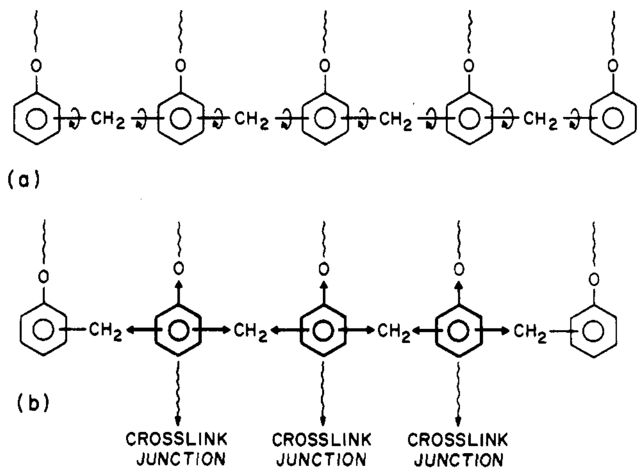

Figure 13. Cross-link junctions in an epoxy–novolac. (a) A reacted polyfunctional monomer unit consists of several nuclei connected by rotatable bonds and therefore is not really a cross-link junction; (b) a cross-link junction is any rigid nucleus with at least three arms connected to the network, in this case the marked nonterminal phenyl rings.

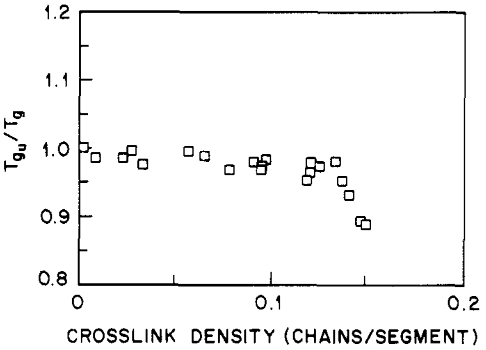

Figure 14. Ratio of the "un-cross-linked" glass transition (from eq 10) to the experimental glass transition of the cross-linked system as a function of cross-link density. DiMarzio's equation (eq 2) predicts that this graph should be linear.

distribution, our binary mixture approximation proved to be reasonable since it predicts correctly the conversion at gelation.

The choice of what we consider to be the "cross-link" deserves some attention. Although one may be tempted to choose a reacted oligomer unit as a multifunctional cross-link junction, this choice is not appropriate for our lattice model, since the cross-link "junction" is actually made of several nuclei connected by rotatable bonds (Figure 13a). We therefore consider a cross-link junction to be any *rigid* nucleus that has at least three arms connected to the network. In our case, the cross-link junctions are the nonterminal benzene rings in the novolac structure when three of their arms are linked to the network (Figure 13b). Hence, all the cross-links in our system are considered to be trifunctional.

In order to test whether the formation of cross-links alone could account for the experimental observations, eq 2 was employed. This equation combines the effects of chain ends and cross-link density. A plot of T_{g_u}/T_g versus X should be linear if eq 2 were to hold. Such a graph is displayed in Figure 14. T_{g_u} was calculated from eq 10. The plot departs from linearity at high conversions, indicating that eq 2 is inadequate. This was to be expected in view of the assumptions and simplifications used by DiMarzio[12] in obtaining this equation, which is strictly valid only for low cross-link densities.

Equation 11 is applicable to high cross-link densities. In order to use this equation with our experimental results

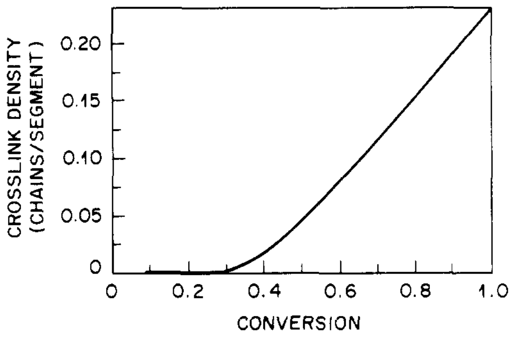

Figure 15. Calculated cross-link density as a function of conversion for a step polymerization between a monomer with number-average functionality of 4.8 and a monomer with number-average functionality of 5.1.[54]

for the epoxy–novolac system, we first recall that $1/T_{g_0} = 0.003\,27$ was obtained from the T_g of the unreacted mixture, and the constant k was determined independently from model monofunctional compounds to be 9.513×10^{-4}. The cross-link density was calculated as discussed in ref 54. We still have two unknown parameters: K_2 and Ψ. These parameters were fitted by using a nonlinear regression program. The values obtained are $K_2 = 0.117$, $\Psi = 37.76$. Figure 8 shows the experimental values of T_g for our epoxy–novolac system and the calculated values from eq 11. An excellent fit is obtained. For the sake of simplificity it was assumed that, for a given cross-link density, the number of segments between any two cross-links is the same. Figure 15 shows the calculated cross-link density as a function of conversion. At the highest measured conversion, the cross-link density is approximately 0.15 elastic chains/segment, that is, there are on the average 6.7 segments on each elastic chain. In reality, however, the problem is much more complex, since the cross-link arms are not symmetric; i.e., an arm that leads from an epoxide to a hardener molecule is longer than an arm leading from one phenyl ring to another within the novolac structure. In fact, the shortest "elastic" chains are composed of only three segments. With chains this short one wonders whether the Gibbs–DiMarzio theory is applicable at all. Actually, the question is whether the lattice model adopted to evaluate the partition function is valid. Certainly the method of evaluating the partition function can be improved, but at a considerable expense of simplicity. However, we agree with DiMarzio in that "the fundamental insight that a drastic decrease in the configurational entropy is the main determinant of glass formation is not likely to be altered".[64] In our simplified approach, the use of the Gaussian functionality is certainly not accurate for the very short chains, but it should be regarded only as a reference point indicating an upper bound given by the configurational entropy of a hypothetical short Gaussian chain. The real short chain has of course a much lower configurational entropy, which is accounted for by an empirical adjustment.

It should be pointed out that one would expect, from eq 11, to see a more pronounced increase in T_g after the gel point, since the cross-link density is zero before the gel point and starts rising immediately thereafter. Some data reported in the literature actually show a break at the gel point in the slope of the T_g versus conversion plot.[29,31,32] In our system, however, we do not observe such a break at the gel point, which occurs at 25% conversion. It could be speculated that the cross-linking contribution may be too small to be detected at low cross-link densities, but that it is still present. In fact, the continuous line in Figure 8, which was generated from eq 11, does not show an

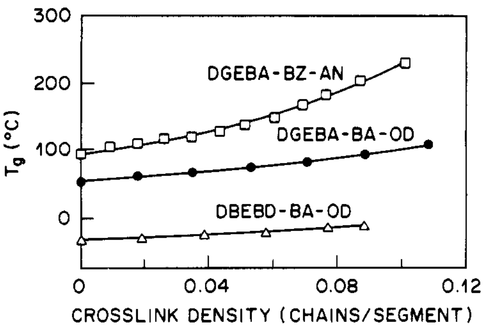

Figure 16. Glass transition as a function of cross-link density for Charlesworth's data.[21] The continuous lines were calculated by using eq 5 with the following parameters (K_2 and Ψ, respectively: DGEBA-BZ-AN 2.11, 21.95; DGEBA-BA-OD 0.98, 21.21; DBEBD-BA-OD 0.80, 16.18; where DGEBA = diglycidyl ether of bisphenol A, BZ = benzidine, AN = aniline, BA = n-butylamine, OD = 1,8 octyldiamine, and DGEBD = diglycidyl ether of butanediol.

obvious break at the gel point, despite the fact that eq 11 contains a term that starts growing at the gel point.

Another possible explanation for not observing a break at the gel point is the fact that in the foregoing analysis we have assumed that the behavior of the experimentally measured T_g parallels that of the thermodynamic glass transition T_2 (at which the configurational entropy is zero[35]). According to the Adam–Gibbs theory,[45] the thermodynamic glass transition T_2 is related to a cooperative region comprising the whole sample. Since after the gel point a new mechanism to restrict entropy is operative (namely, the formation of elastically effective cross-links), one would expect to see a change in the behavior of T_2 immediately after the gel point. The fact that such behavior is not observed in our T_g data may be due to the fact that the experimentally observed T_g is a relaxational phenomenon associated with a relatively small number of segments and therefore is not sensitive to gelation.

It is noteworthy that the plot of ΔC_p (a true thermodynamic property) versus conversion (Figure 9) shows approximately constant values below the gel point (25%), and a decrease thereafter. Since ΔC_p has been shown to be intimately related to configurational terms,[65] its decrease after the gel point is consistent with the expected drop in configurational entropy as effective cross-links are formed. Nevertheless, more work is needed to prove that this is not a fortuitous situation.

Application to Other Systems. Our model fits Charlesworth's experimental data[21] adequately (Figure 16). These data had been obtained from completely reacted epoxy–amine systems, in which the cross-link density had been varied by changing the ratios of cleverly chosen reacting species. Equation 11 can also be used to fit successfully Feger's data,[29] which consist of a hydroxyl-terminated poly(propylene oxide) cross-linked with a trifunctional isocyanate. The gel conversion of this system is ~0.71. The pregel region can be described by eq 10, with $1/T_{g_0} = 0.0049$ and $k = 6.118 \times 10^{-4}$. In the postgel region, the influence of the cross-links can be taken into consideration by using eq 11. Since the molecular weight between cross-links is not too small, the correction for non-Gaussian behavior can be ignored, so $\Psi = 0$ in eq 11. A value for K_2 of 2.096 gives a very good fit of eq 11 to the data of Feger and MacKnight (Figure 17).

In principle, eq 11 could also be applied to nonstoichiometric systems. In this case T_{g_0} would be a function of the stoichiometric imbalance, and ξ should be the conversion of the limiting reagent. The stoichiometric imbalance would also alter the cross-link density X. It is expected that the constants K_2 and Ψ would not vary with the stoichiometry, but so far there is no experimental evidence to support this.

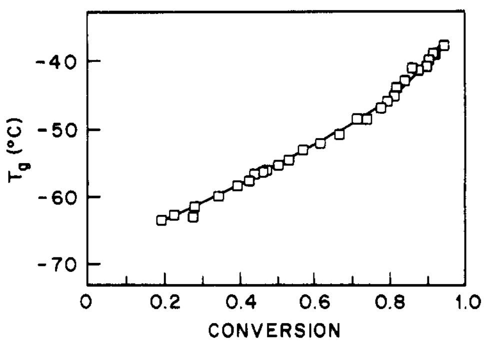

Figure 17. Glass transition data from Feger and co-workers[29] for a system consisting of α,ω-dihydroxypolypropylene oxide and a trifunctional isocyanate. The continuous line was calculated by using eq 11.

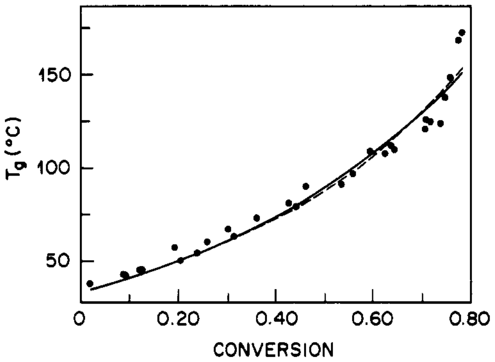

Figure 18. Havlicek and Dusek's[6] equation (eq 16) fit to our data with $T_{g_1} = 504$ K and $C = 5.5 \times 10^{-4}$ (continuous line). The dashed line is DiBenedetto's[13] equation (eq 1) fit to our data by using conversion ξ instead of cross-link density x and T_{g_0} instead of T_{g_u}, with $\epsilon_\infty/\epsilon_0 = 0.55$ and $c_\infty/c_0 = 0.31$.

Even though eq 11 allows us to obtain good empirical fits to other data from the literature,[24,25,27,28,31,32] this equation in its present form is not strictly correct for partially reacted epoxy–amine systems. In this case eq 10 is no longer valid, since now we have three different kinds of chain ends: epoxides, primary amines, and secondary amines. Equation 10 would now become

$$1/T_{g_u} = 1/T_{g_0} - k_1\xi_1 - k_2\xi_2 \qquad (15)$$

where ξ_1 would be the overall conversion of epoxides, and ξ_2 the conversion of primary amines. Therefore, comparing with eq 10, a new constant needs to be introduced. Although this extra constant would certainly enable us to *fit* the data, we would rather see k_1 and k_2 values in eq 15 independently obtained from model compounds and then use these values in combination with eq 5 to describe cross-linking systems. The data presently available in the literature are not abundant enough to allow this.

Comparison with Other T_g versus Conversion Relationships. Havlicek and Dusek[6] have used the following empirical equation to fit data reported in the literature:

$$1/T_g = (1 - \xi)/T_{g_0} + \xi/T_{g_1} + C\xi(1 - \xi) \qquad (16)$$

where T_{g_1} is the glass transition temperature at full conversion ($\xi = 1$) and C is an adjustable parameter. Figure 18 shows the best fit of eq 16 to our data using T_{g_1} and C as adjustable parameters. Although the fit is in general good, it fails to predict the very sharp upturn in T_g at high conversions.

As mentioned in the Introduction, a modified form of DiBenedetto's equation[13] (eq 1) has been widely used in the literature to fit T_g versus conversion data.[26,28,29] The modification consists of using conversion ξ instead of cross-link density x and T_{g0} (T_g at $\xi = 0$) instead of T_{g_u}. The best fit of this modified form of eq 1 to our data is shown in Figure 18. As in the previous case, a good overall fit is obtained, but the T_g values at high conversions are underpredicted by ~20 °C. On the other hand, if we use the unmodified DiBenedetto equation (eq 1), and take into account the variation of T_{g_u} with conversion through eq 10, an excellent fit is obtained. This is conceptually the same approach as that of Stutz and co-workers[24] although there are three differences: (i) instead of using eq 10, these researchers employed an equation based on Fox–Flory's relation (eq 6), (ii) their cross-link density is based on total number of junction points rather than on elastically effective cross-links, and (iii) they have reduced the number of parameters by assuming that c_∞/c_0, the ratio of segmental mobilities between the cross-linked and the uncross-linked system, is zero. Their equation is

$$T_g = (T_{g_\infty} - k_1(1-\xi))[1 + k_2\,(X_c/(1-X_c))] \qquad (17)$$

where T_{g_∞} is the reference true backbone glass temperature, k_1 a constant characterizing the influence of end groups on T_g, k_2 another constant characterizing the influence of cross-links, and X_c the cross-link density. Any junction with a functionality of three or higher is considered to be a cross-link, and the higher functional cross-links are weighted more heavily than the lower functional cross-links. In our chemical system the number of junctions is proportional to the conversion if we assume that all the groups are equally reactive. At full conversion, every f-functional monomeric unit will have f-2 trifunctional junctions (Figure 13b). Dividing the number of junctions in an epoxy–novolac repeat unit at full conversion by the number of segments in this repeat unit yields a value of 0.128 (for our particular chemical system), which is the proportionality constant between X_c and ξ (i.e., $X_c = 0.128\xi$).

Figure 19 shows a least-squares fit of eq 17 to our data using T_{g_∞}, k_1, and k_2 as adjustable parameters. This equation fails to fit accurately the data at very high as well as very low conversions.

An equation very similar in form to DiBenedetto's had been derived earlier by Fox and Loshaek[11] using free volume arguments. This equation can be expressed as[54]

$$T_g = T_{g_u} + aX/(1 - bX) \qquad (18)$$

where a and b are constants. Unfortunately this equation has been overlooked in the literature, since most researchers have used its simplified (though less general) version

$$T_g = T_{g_u} + aX \qquad (19)$$

which holds only for high molecular weights of the linear chains and low cross-link density.

The "forgotten" Fox and Loshaek equation (eq 18) fits our data very well with $a = 2.26$, $b = 1.23$, and with eq 13 to evaluate T_{g_u}. The fit is indistinguishable from that shown in Figure 8.

On the basis of entropic considerations applied to a model of the thermosetting polymer consisting of a random mixture of a fully reacted network with the initial monomers, Pascault and Williams have derived the following equation:[23]

$$(T_g - T_{g_0})/(T_{g_1} - T_{g_0}) = \lambda\xi/(1 - (1 - \lambda)\xi) \qquad (20)$$

where $\lambda = \Delta C_{p_1}/\Delta C_{p_0}$, the subindex 0 represents the unreacted system ($\xi = 0$), and the subindex 1 represents the fully reacted network ($\xi = 1$). If the values of ΔC_{p_0}, ΔC_{p_1}, T_{g_0}, and T_{g_1} are known, no adjustable parameters are required.

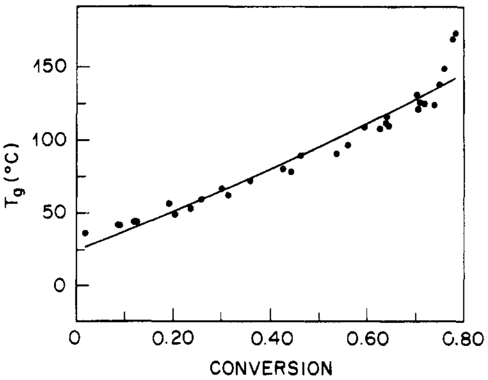

Figure 19. Stutz's[24] equation (eq 17) fit to our data, with T_{g_∞} = 337 K, k_1 = 39.3, k_2 = 2.37.

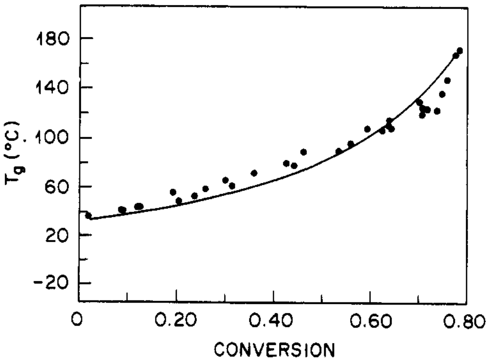

Figure 20. Pascault and Williams'[23] equation (eq 21) fit to our data.

Since full conversion could not be achieved with our system, T_{g_1} and ΔC_{p_1} are not known. Although one could obtain these values from extrapolation from Figures 8 and 9, this was not attempted, since our objective was to test the predictive capabilities of this equation with the minimum possible amount of experimental data. Instead of using hypothetical data from a fully reacted network, we used data from the polymer with the highest conversion we could measure, $\xi_M = 0.78$. Assuming that the polymer at any conversion can be modeled as a random mixture of this $\xi_M = 0.78$ polymer with monomer, then eq 20 can be restated as

$$(T_g - T_{g_0})/(T_{g_M} - T_{g_0}) = \lambda'\xi'/[1 - (1 - \lambda')\xi'] \qquad (21)$$

where $\xi' = \xi/\xi_M$, $\lambda' = \Delta C_{pM}/\Delta C_{p0}$, the subindex M represents the polymer with the highest measured conversion, and the subindex 0 represents the unreacted material.

Using the experimental values T_{g_0} = 33 °C, ξ_M = 0.78, T_{g_M} = 173 °C, ΔC_{p_0} = 0.1 cal/g °C, ΔC_{p_M} = 0.03 cal/g °C, one can construct the curve shown in Figure 20. Although the fit is not as good as that obtained with eq 11, it is still reasonable, in particular if one bears in mind that it was not necessary to (i) use adjustable parameters, (ii) take experimental data from model monofunctional compounds, or (iii) make statistical calculations assuming a particular model for the network buildup. It should be kept in mind, however, that the goodness of the fit is due in part to the fact that the curve is forced to pass through T_{g_M}. (All the other fits we have shown here are "free fits", where the curves were not forced to pass through T_{g_M}.)

Conclusions

A simple equation to model the change in glass transition temperature with extent of reaction in highly cross-linked thermosetting systems has been derived. The model assumes that the increase in T_g is caused by (a) decrease in chain-end concentration, (b) formation of effective cross-links, and (c) further decrease in the configurational entropy due to departure from Gaussian behavior at high cross-link densities. With this equation, it is possible to *predict* the changes in the glass transition of a thermosetting system at low conversions by using independently obtained data from model monofunctional compounds. The increase in T_g at higher conversions can be fitted by taking into account the drop in configurational entropy brought about by the formation of cross-links. Since the size of the chains between cross-links at high conversions is only a few bonds, it was necessary to include in the model the deviation caused by non-Gaussian behavior and steric effects. This deviation was accounted for in an empirical way in order to obtain a simple equation.

This model successfully describes data reported here for a polyfunctional epoxy–novolac system. Our data cannot be fitted as accurately by other equations published in the literature unless T_{g_u}, the glass transition of the uncross-linked polymer, is allowed to vary with conversion in order to account for the decrease in chain ends, *and* two parameters are used to describe the influence of the cross-links.

Further work is being carried out to determine the relative importance of junction points versus effective crosslinks in relation to the glass transition temperature.

Acknowledgment. We gratefully acknowledge the discussions held with Dr. Shiro Matsuoka and the comments of Dr. Herbert Stutz, as well as one of the reviewer's very thorough and helpful review. A.H. and C.W.M. also acknowledge grants from the Army Research Office (Grant DAAG29-83-K-0149) and from the Office of Naval Research (Grant N00014-88-K-0366). The solid-state NMR spectra were obtained by the Colorado State University NMR Center, funded by the National Science Foundation Grant CHE-8616437.

References and Notes

(1) Horie, K.; Hiura, H.; Sawada, M.; Mita, I.; Kambe, H. *J. Polym. Sci., Part A-1* **1970**, *8*, 1357.
(2) Lunak, S.; Vladyka, J.; Dusek, K. *Polymer* **1978**, *19*, 931.
(3) Gillham, J. K. *Polym. Eng. Sci.* **1979**, *19*, 676.
(4) Bair, H. E.; Ludwick, A. G. *Bull. Am. Phys. Soc.* **1984**, *29*, 244; Proceedings, 13th North American Thermal Analysis Society Annual Meeting, Sept 23–26, 1984, Philadelphia, PA; 1984; p 224.
(5) Huguenin, F. G.; Klein, M. T. *Ind. Eng. Chem. Prod. Res. Dev.* **1985**, *24*, 166.
(6) Havlicek, I.; Dusek, K. In *Crosslinked Epoxies*; Sedlacek, B., Kahovec, J., Eds.; Walter de Gruyter & Co.: Berlin, 1987; p 417.
(7) Matsuoka, S.; Quan, X.; Bair, H. E.; Boyle, D. J. *Macromolecules* **1989**, *22*, 4093.
(8) Bidstrup, S. A.; Macosko, C. W. In *Crosslinked Epoxies*; Sedlacek, B., Kahovec, J., Eds.; Walter de Gruyter & Co.: Berlin, 1987; p 253; *J. Polym. Sci., Part B: Polym. Phys.* **1990**, *28*, 691.
(9) Hale, A.; Macosko, C. W. *Proc. Polym. Mater. Sci. Eng.* **1988**, *59*, 1196.
(10) Shimbo, M.; Ochi, M.; Arai, K. *J. Coat. Technol.* **1984**, *56*(713), 45.
(11) Fox, T. G.; Loshaek, S. *J. Polym. Sci.* **1955**, *15*, 371.
(12) DiMarzio, E. A. *J. Res. Natl. Bur. Std., Sect. A* **1964**, *68A*, 611.
(13) DiBenedetto, A. T. "unpublished results", as cited by: Nielsen, L. E. *J. Macromol. Sci., Rev. Macromol. Chem.* **1969**, *C3*(1), 69.
(14) Chompff, A. J. In *Polymer Networks, Structure and Mechanical Properties*; Chompff, A. J., Newman, S., Eds.; Plenum Press: New York, 1981; p 145.
(15) Becker, R. *Plaste Kautsch.* **1973**, *20*, 809; **1975**, *22*, 790.
(16) Rietsch, F.; Daveloose, D.; Froelich, D. *Polymer* **1976**, *17*, 859.
(17) Ponomareva, T. I.; Irzhak, V. I.; Rozenberg, B. A. *Polym. Sci. USSR (Engl. Transl.)* **1979**, *20*, 673.
(18) Banks, L.; Ellis, B. *Polymer* **1982**, *23*, 1466.
(19) Lee, G.; Hartman, B. *J. Appl. Polym. Sci.* **1983**, *28*, 823.
(20) Bellenger, V.; Verdu, J.; Morel, E. *J. Polym. Sci., Part B: Polym. Phys.* **1987**, *25*, 1219.
(21) Charlesworth, J. M. *J. Macromol. Sci., Phys.* **1987**, *B26*(1), 105.
(22) DiBenedetto, A. T. *J. Polym. Sci., Part B: Polym. Phys.* **1987**, *25*, 1949.
(23) Pascault, J. P.; Williams, R. J. J. *J. Polym. Sci., Part B: Polym. Phys.* **1990**, *28*, 85.
(24) Stutz, H.; Illers, K. H.; Mertes, J. *J. Polym. Sci., Part B: Polym. Phys.* **1990**, *28*, 1483.
(25) Barton, J. M. *J. Macromol. Sci., Chem.* **1974**, *A8*(1), 25; *Polymer* **1980**, *21*, 603.
(26) Adabbo, H. E.; Williams, R. J. J. *J. Appl. Polym. Sci.* **1982**, *27*, 1327.
(27) Riccardi, C. C.; Adabbo, H. E.; Williams, R. J. J. *J. Appl. Polym. Sci.* **1984**, *29*, 2481.
(28) Enns, J. B.; Gillham, J. K. *J. Polym Sci.* **1983**, *28*, 2567.
(29) Feger, C.; MacKnight, W. J. *Macromolecules* **1985**, *18*, 280. Feger, C.; Chambon, F.; Winter, H.; MacKnight, W.; Dusek, K. *Tech. Pap.—Soc. Plast. Eng.* **1988**, *34*, 1054.
(30) Bair, H. E. *Polym. Prepr. (Am. Chem. Soc., Div. Polym. Chem.)* **1985**, *26*, 10.
(31) Pang, K. P.; Gillham, J. K. *J. Appl. Polym. Sci.* **1989**, *37*, 1969.
(32) Yu, W. C.; Sung, C. S. P. *Macromolecules* **1988**, *21*, 365.
(33) Couchman, P. R. *J. Mater. Sci.* **1980**, *15*, 1680; *Macromolecules* **1980**, *13*, 1272.
(34) Aronhime, M. T.; Gillham, J. K. *J. Coat. Technol.* **1984**, *56*(718), 35.
(35) Gibbs, J. H.; DiMarzio, E. A. *J. Chem. Phys.* **1958**, *28*, 373.
(36) DiMarzio, E. A.; Gibbs, J. H. *J. Chem. Phys.* **1958**, *28*, 807.
(37) Flory, P. J. *Statistical Mechanics of Chain Molecules*; Interscience: New York, 1969; Chapter VIII.
(38) Kuhn, W.; Grün, F. *Kolloid-Z.* **1942**, *101*, 248. Kuhn, W.; Kuhn, H. *Helv. Chim. Acta* **1943**, *26*, 1394. Kuhn, W. *Helv. Chim. Acta* **1946**, *29*, 1095.
(39) Treloar, L. R. G. *The Physics of Rubber Elasticity*, third ed.; Clarendon Press: Oxford, 1975; Chapter 6.
(40) Hill, J. L.; Stepto, R. F. *Trans. Faraday. Soc.* **1971**, *67*, 3202.
(41) Mark, J. E.; Curro, J. G. *J. Chem. Phys.* **1983**, *79*, 5705.
(42) Charlesworth, J. M. *Polym. Eng. Sci.* **1988**, *28*, 230.
(43) Macosko, C. W.; Miller, D. R. *Macromolecules* **1976**, *9*, 199.
(44) Boyer, R. F. *Rubber Chem. Technol.* **1963**, *36*, 1303.
(45) Adam, G.; Gibbs, J. H. *J. Chem. Phys.* **1965**, *43*, 139.
(46) Fox, T. G.; Flory, P. J. *J. Appl. Phys.* **1950**, *21*, 581; *J. Polym. Sci.* **1954**, *14*, 315.
(47) Ueberreiter, K.; Kanig, G. *J. Colloid Sci.* **1952**, *7*, 569.
(48) Roovers, J. E. L.; Toporowski, P. M. *J. Appl. Polym. Sci.* **1974**, *18*, 1685.
(49) Meares, P. *Polymers, Structure and Bulk Properties*; Van Nostrand: London, 1965; p 265; *Trans. Faraday Soc.* **1957**, *53*, 31.
(50) Roovers, J. E. L.; Bywater, S. *Macromolecules* **1972**, *5*, 384.
(51) Worsfold, D. J.; Zillioux, J. G.; Rempp, P. *Can. J. Chem.* **1969**, *47*, 3379.
(52) Weiss, P.; Hild, G.; Herz, J.; Rempp, P. *Makromol. Chem.* **1970**, *135*, 249.
(53) Cook, W. D. *Eur. Polym. J.* **1978**, *14*, 715.
(54) Hale, A. Ph.D. Thesis, University of Minnesota, 1988.
(55) Langley, N. R.; Polmanteer, K. E. *J. Polym. Sci., Polym. Phys. Ed.* **1974**, *12*, 1023.
(56) Miller, D. R.; Macosko, C. W. *Macromolecules* **1976**, *9*, 206.
(57) Helfand, D.; Villani, T. *Proceedings, 14th Electrical/Electronics Insulation Conference*, Oct 8–11, 1979; IEEE 79CHI510-7-EI; 1979; p 290.
(58) Hale, A.; Macosko, C. W.; Bair, H. E. *J. Appl. Polym. Sci.* **1989**, *38*, 1253.
(59) Struik, L. C. E. *Physical Aging in Amorphous Polymers and Other Materials*; Elsevier: New York, 1978.
(60) Matsuoka, S.; Bair, H. E. *J. Appl. Phys.* **1977**, *48*, 4058.
(61) Rozenberg, B. A. *Adv. Polym. Sci.* **1986**, *75*, 113.
(62) Reid, R. C.; Prausnitz, J. M.; Sherwood, T. K. *The Properties of Gases and Liquids*, 3rd ed.; McGraw-Hill: New York, 1977; 261.
(63) Oleinik, E. F. *Pure Appl. Chem.* **1981**, *53*, 1567; *Adv. Polym. Sci.* **1986**, *80*, 49.
(64) DiMarzio, E. A. *Ann. N.Y. Acad. Sci.* **1981**, *371*, 1.
(65) DiMarzio, E. A.; Dowell, F. *J. Appl. Phys.* **1979**, *50*, 6061.

Registry No. MPPP, 125107-96-2; (Araldite ECN-1273)(Araldite HT 9490) (copolymer), 132801-87-7.